Decolorization of Acid Dye Useing Sono-Based Processes: Sonoelectrochemical, Sonophotoelectrochemical and Sonophotoelectro-Catalysis

M. E. Olya[1*], A. Pirkarami[2], M. Soleimani[3] and N. Yousefi Limaee[4]

[1.] Assistant Professor, Department of Environmental Research, Institute for Color Science and Technology, P. O. Box: 16765-654, Tehran, Iran.

[2.] M. Sc., Department of Environmental Research, Institute for Color Science and Technology, P. O. Box: 16765-654, Tehran, Iran.

[3.] Assistant Professor, Department of Chemistry, Faculty of Science, Imam Khomeini International University, P. O. Box: 288, Qazvin, Iran.

[4.] M. Sc., Department of Environmental Research, Institute for Color Science and Technology, P. O. Box: 16765-654, Tehran, Iran.

ARTICLE INFO

ABSTRACT

In recent years, combinatorial methods have attracted a great deal of attention. Among them, sono-combining techniques have shown a significant potential as an economic technology applicable and environment-friendly technology for wastewater treatment. In this study, Sono Electrochemical (SE), Sono Photo Electrochemical (SPE) and Sono Photo Electro Catalytic (SPEC) techniques were investigated for decolorization of Acid Red 88 (AR88). It was found that SPEC is capable of decolorizing AR88 entirely after 35minutes by using Ni-TiO$_2$ as a catalyst with higher efficiency than SPE and SE techniques. The results are also shown that SPE had more yield than SE because in the case of SPE, the process was performed not only by sonolysis but also by photoelectrolysis. Furthermore, initial concentration of dye, initial pH, current density and concentration of supporting electrolyte were investigated and the optimum conditions were obtained. Based on the obtained results, SPEC is an appropriate technology for decolorizing of acid dyes completely with a faster rate. Photocatalyst efficiency was evaluated using SEM and XRD techniques. The characterization of the post-treated product using HPLC studies revealed intermediate compounds. Prog. Color Colorants Coat. 7(2014), 105-120© Institute for Color Science and Technology.

1. Introduction

The dye stuff lost in the textile industry poses a major problem to wastewater sources [1]. From the environmental point of view, a wide variety of complex chemicals has been entered in wastewaters via dyeing

---

*Corresponding author: olya-me@icrc.ac.ir

process causing major pollution problems. Whereas discharge of polluted wastewater in streams of water will damage the ecosystem and aquatic life, various practical strategies have been applied to treat industrial wastes for preserving more viable water resources [2, 3]. As an environmental issue, azo dyes and their degraded products have received the most attention due to high impact of derogatory, mutagenic property, extensive use, high potential to form toxic aromatic intermediates and their low removal proportion during primary and secondary treatment stages [4, 5]. However, 10–15% of azo dyes are lost during the dyeing procedures and released as contaminant in effluent [6, 7]. Hence, it is mandatory to develop effective remediation technologies for these compounds. As, the nature of textile wastewater depends on technical, technological, social and cost-effective factors, seeking for appropriate treatment methods are continuing in research and development centers.

Conventional chemical (e.g. coagulation-flocculation) and biological (e.g. activated sludge, successive bed reactors, anaerobic/anoxic) processes are widely used for textile wastewater treatment, however, with a rather limited success [3,8]. Since, the textile dyes are deliberately designed to resist biological, photolytic and chemical decolorization, conventional treatment systems cannot achieve relevant extent of decolorization.

Nowadays, photocatalytic processes using nano metal oxide as a catalyst have attracted *excess* consideration for various environmental applications for decomposing organic contaminants into simple inorganic species [9]. Nevertheless, the shortcoming of photocatalytic process is the rapid recombination of electron–hole pairs that is caused by oxidation and reduction reactions on the same photocatalyst particle [10]. This phenomenon creates a short-circuit electron transfer and accelerates the recombination and lowers the removal efficiencies and quantum yield. For these reasons, several novel methods have been applied to increase the photocatalytic

efficiencies such as electro-assisted and ultrasonic-assisted photocatalysis. In all these cases, they have been shown to be able to improve the photocatalytic efficiency to a great extent [11-14]. For instance, the synergetic effect of UV light and electric field showed a better result on the decolorization of dye in photoelectrochemical methods [15]. By the application of external bias voltage to photocatalytic process, the photocatalyst acts as photoanode and an external anodic bias is applied to drive the photogenerated electrons and holes in opposing directions so that the charge recombination is retarded [16, 17]. Also, sonolysis has been reported to be able to greatly improve the photocatalytic efficiency [18].

In this study, the effect of sonolysis in electrochemical, photoelectrochemical and photoelectro-catalysis methods was investigated to determine the various and positive effects of three combined systems on decolorization of AR88. Also, the effect of operating conditions such as pH, current density, initial concentration of dye, supporting electrolyte and temperature were studied in three systems including SE, SPE and SPEC techniques. The efficiency of the photocatalyst was studied using SEM and XRD techniques. The post-treatment product was also characterized using HPLC techniques.

2. Experimental

2.1. Materials and apparatus

Acid Red 88 (purity≤98%) was purchased from Ciba Ltd. And used without further purification. The chemical structure of this dye is shown in Figure 1.

The chemicals used in this study were titanium tetraisopropoxide (TTIP), Nickel nitrate hexahydrate, diethanolamine, glacial acetic acid, absolute alcohol, and deionized water. All the chemical reagents (purchased and used as received from Merck chemical company in Germany) were of analytical grade or better quality.
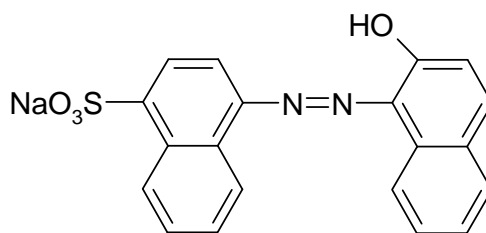

Figure 1: Chemical structure of AR88.

The pH of the solutions was adjusted by adding a small amount of 2 M H_2SO_4 or NaOH. . The electrolyte was NaCl, which was also purchased from Merck. This salt has negligible effect on pH and is non-toxic, inexpensive, soluble, and highly conductive. Distilled water was employed as a solvent.

Decolorization of dye solutions was checked by measuring the absorbance of dye solutions at different intervals using M 350- double beam UV-Vis spectrophotometer model of campec covering the 400-800 nm wavelength range.

The process of ultrasound (US) irradiation was performed with a KS-250 ultrasonic generator. A 6 W UV lamp with central wavelength of 253.7 nm was used to attain the UV light illumination. Ni–TiO$_2$ catalyst was prepared and applied in suspension. Scanning electron microscope (SEM) image of Ni-TiO$_2$ was obtained using HITACHI Model 3000 SH, Japan. X-ray diffraction (XRD) of synthesized catalyst was prepared by Philips PW 1710 high power diffractometer (the Netherlands) with $Cu_{K\alpha}$ radiation at 40 kV and 40 mA. The high performance liquid chromatographic analysis was carried out in a Shimadzu SCL-10AVP apparatus equipped with a diode array detector. Chromatographic analysis was performed using a high-performance liquid chromatograph (HPLC, Knauer, Germany) coupled with a UV 2600 diode-array detector (DAD) and a Smart Line 1000 pump. The separation column was ODS-C18 (5 pm, 4.6 mm X 250 mm) having a precolumn of the same material, 1 cm long. A mixture of acetonitrile and water, 60:40 (v/v), was used as the mobile phase at a flow rate of 0.7 mL min^{-1} at room temperature. For photolysis, aliquots of approximately 2 mL were taken out at specific time intervals: 0 (before treatment), 10, 20, 30, and 60 min. during decolorization. Injections were carried out at 20 μ. Standard dye (50 mg L^{-1}) was separately injected to the HPLC device to determine its retention time.

2.2. Preparation of photocatalyst

For the preparation of Ni-TiO$_2$ nano photocatalyst, the components of the nano-sized powder were synthesized separately and then mixed to form Ni-TiO$_2$ nano particles. TiO$_2$ was firstly synthesized by dissolving hydroxylpropyl cellulose (HPC) in ethanol begin rapid stirring for 5 min. After that, TTIP was added to the mixture and stirred for 15 min. Subsequently, a mixture of glacial acetic acid, absolute alcohol and deionized water was added and stirred for 15 min to obtain a yellow transparent acidic TiO$_2$ sol. The sol was allowed to stand for 30 min at room temperature.

For the preparation of nickel sol, nickel nitrate hexahydrate was at first dissolved in absolute alcohol and stirred for 5 min. Then, a mixture of diethanolamine, absolute alcohol and deionized water was poured into the solution under rapid stirring. The resulting solution was continuously stirred for 15 min to achieve a transparent alkaline nickel sol.

For the final Ni-TiO$_2$ photocatalyst, the Ni sol was directly incorporated into the TiO$_2$ sol. The resultant nanocomposite was allowed to dry at room temperature. Then, it was calcined at 350 °C for 10 min and subsequently at 500 °C for 5 hours (The temperature was increased with a rate of 5 °C/sec).

2.3. Experimental procedure

Batch reactors made of quartz as shown in Figure 2 which were used to examine the effect of SE, SPE and SPEC methods on decolorization of AR88.

The magnetic stirrer was used for circulating solutions and the temperature was maintained at 25 °C. The reactor in Figure 2(a) is designed for sonoelectrochemical process consist of ultrasound generator, feeding supply and two rectangular electrodes (steel 316 L) with the surface area of 20×200 mm^2. In reactor (b), a 6 W UV lamp is added to study the synergistic effect of photo on sonoelechtrochemical process. The effect of catalyst is investigated in a slurry operation using Ni-TiO$_2$ catalyst (Figure 2(c)). Before and after each run, the electrodes were thoroughly washed with water, placed in HCl solution for at least 15 minutes, and then washed with water again. In all cases, the reactor with the dimension of 29 cm×7 cm×7.5 cm and 1 L volume potential for solutions is applied.

The experiments were carried out at pH 9, current density of 100 Am^{-2}, dye concentration of 30 mg L^{-1}, supporting electrolyte amount of 15 mg L^{-1}, ultrasound power of 55 mW mL^{-1} and temperature of 25 °C.

Maximum absorption wavelength (505 nm) is used to determine the absorption decrease of dye at different time intervals, using a UV-Vis spectrophotometer. The standard calibration curves were used to estimate the percentage of dye decolorization.
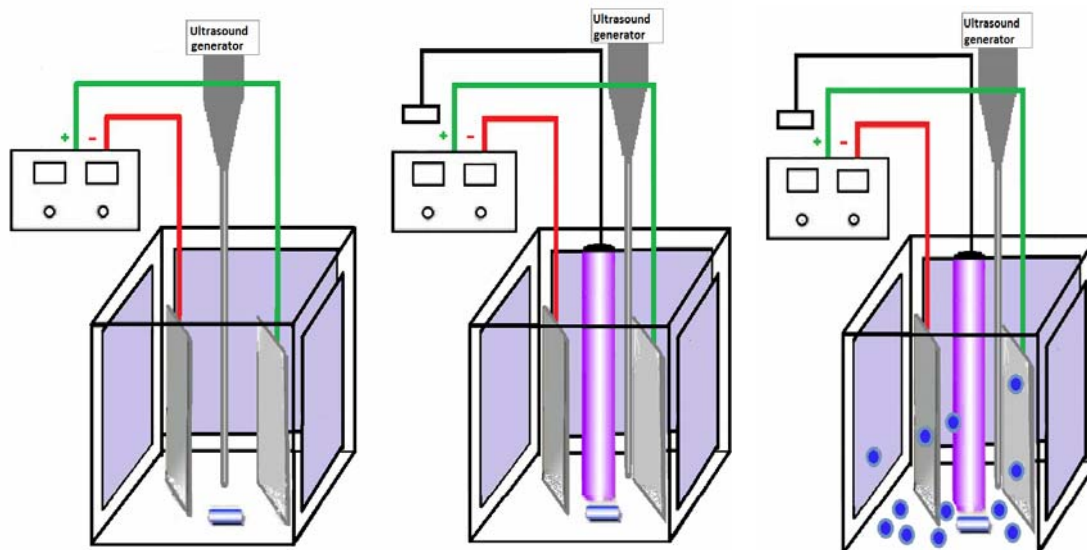
Figure 2: The schematic of different kinds of reactor (a) SE reactor, (b) SPE reactor, and (c) SPEC reactor**.**

The efficiency of dye decolorization was examined according to Eq. (1)

$$R = \frac{C_0 - C_t}{C_0} \times 100 \qquad (1)$$

where C_0 is the initial concentration of dye, and C_t is the concentration of dye after treatment with SE, SPE and SPEC processes.

It should be noted that the experiments were also carried out by applying UV irradiation alone and the results showed no significant change in decolorization of dye (the corresponding data is not presented).

3. Results and discussion

3.1. Performance of different used methods

To investigate the application of SE, SPE and SPEC reactors and obtaining the overview to continue the study, experiments were carried out at concentration of 30 mg L^{-1} in a one-liter reactor for 35 minutes using steel as anode and cathode. At the end of each experiment, the samples were centrifuged and the dye concentration was determined. Figure 3 shows the effect of different reactors on the percentage of dye removal. As shown in this figure, there is a superior effect on dye decolorization in the case of incorporative processes.

3.2. Effect of current density

To study the effect of current density on decolorization of AR88 at different methods including SE, SPE and SPEC, experiments were performed at various current densities (25, 50, 80 and 100Am^{-2}). Steel was used as anode and cathode and Ni-TiO$_2$ catalyst with the concentration of 0.03 g L^{-1} was applied in the practice. Experiments were carried out at 1000 mL of the dye solution with the concentration of 30 mg L^{-1} at pH=9 for 35 min. NaCl with the concentration of 15 mg L^{-1} was used as the supporting electrolyte.
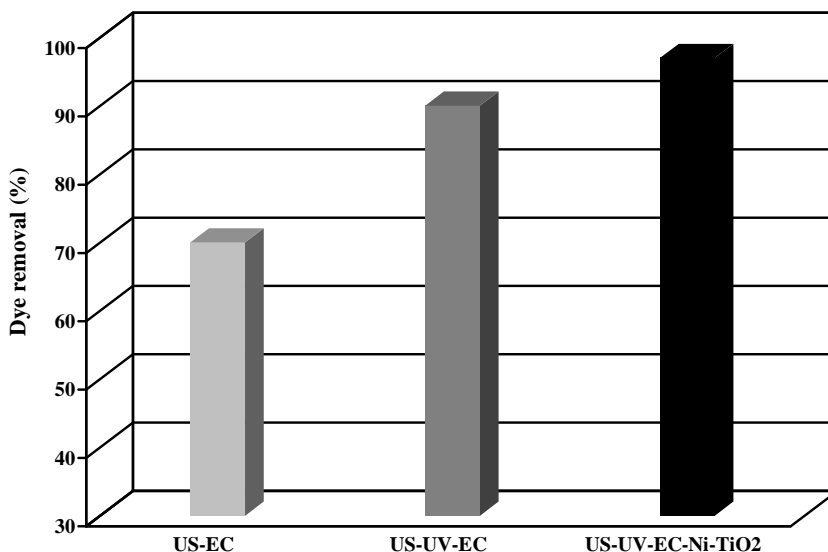
Figure 3: The effect of different methods on decolorization of AR88.

As shown in Figure 4, in the plot of decolorization efficiency versus time, a sharp ascending plot was observed after 5 min of decolorization in all cases of SE, SPE and SPEC for different current densities of 25, 50, 80 and 100Am^{-2}. Results show that lower current density leads to lower decolorization efficiency and longer time is required to attain equilibrium. Figure 4(a) shows the decolorization percentage of 78% for the current densities of 80 and 100Am^{-2} by the SE reactor after 35 min. Whereas Figure 4(b) shows the decolorization efficiency of 93% after 35 min for the current density of 80 and 100 Am^{-2}. The amount of 98% was obtained in similar condition in the case of SPEC (Figure 4(c)).
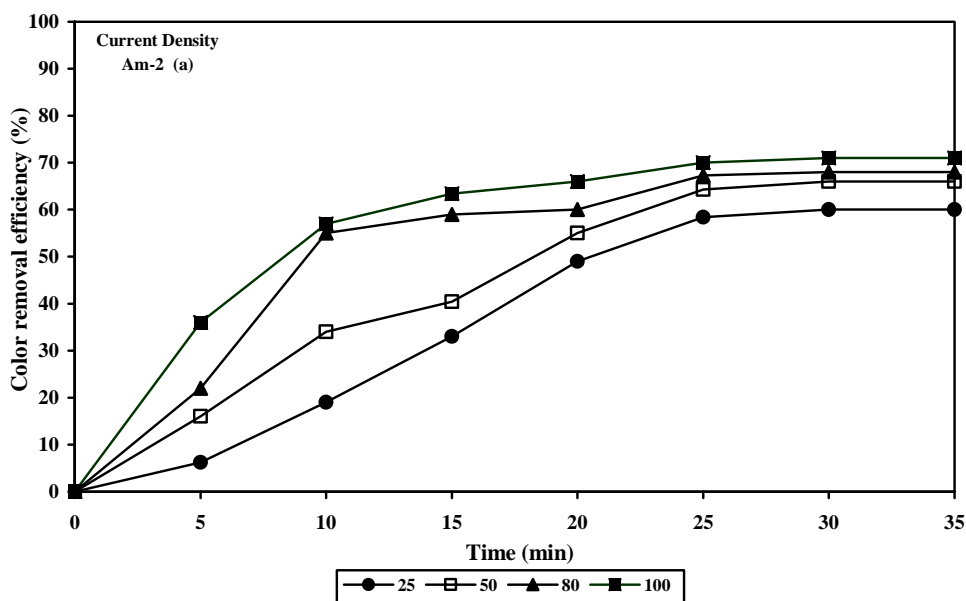

Figure 4: Effect of current density on the decolorization of AR88 for (a) SE, (b) SPE and (c) SPEC.
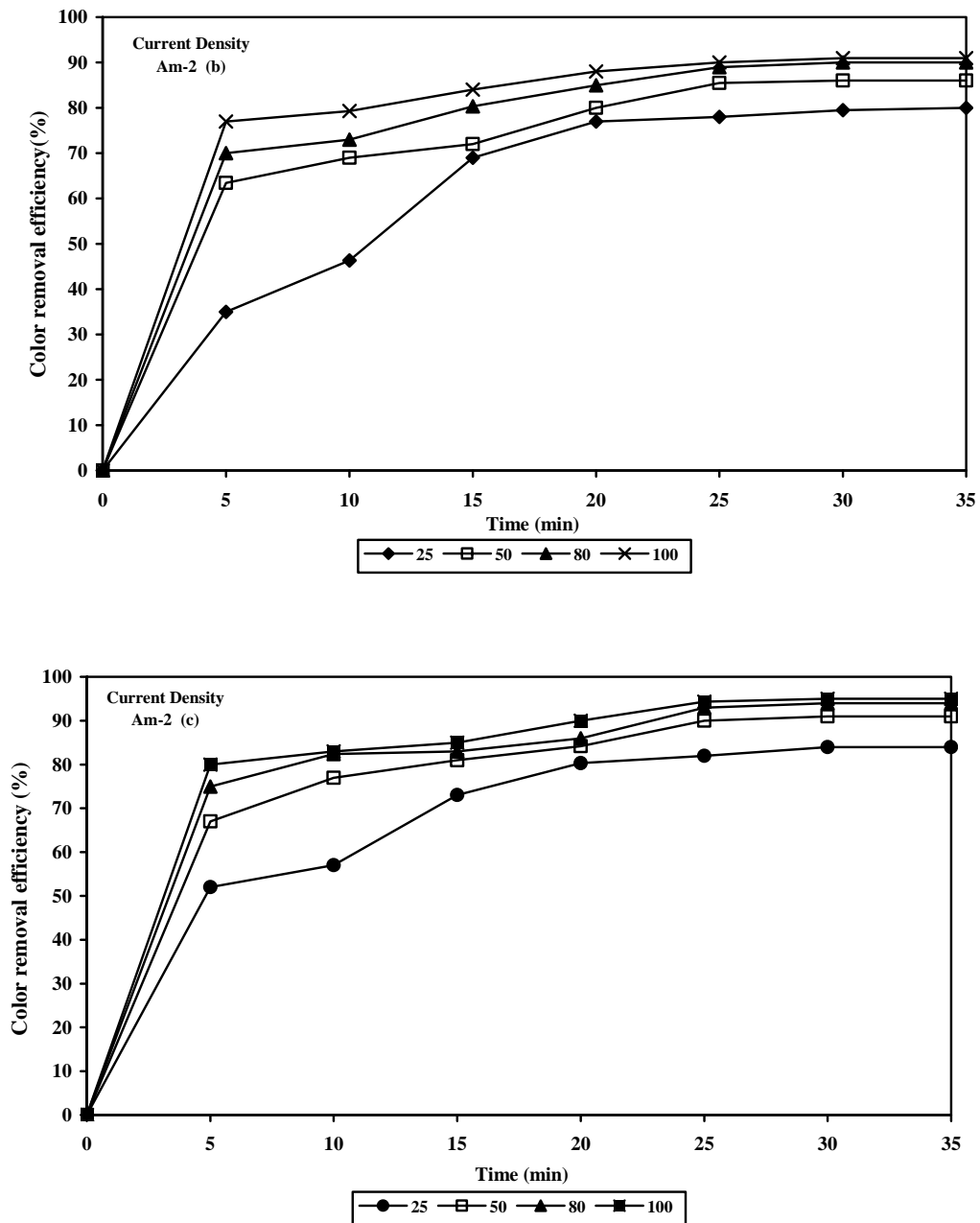
Figure 4: Continued.

In this case, the decolorization of AR88 was studied in the presence of heterogeneous (Ni-TiO$_2$) photoelectro catalysts that seems to be the essential agent in removal efficiency. Applied current through the electrodes has two distinct effects. On one hand, it accelerates the dividing of electron-hole pairs and produce additional oxidative species. On the other hand, the applied positive potential on the electrodes may increase the adsorption of AR88 on Ni-TiO$_2$ which enhances decolorization efficiency to some extent [19, 20].

3.3. Effect of Initial pH

The influence of pH (in the range of 3–11) on the decolorization rate of AR88 was inspected in dye concentrations of 30-250 mg L⁻¹ and the presence of NaCl (5-20 mg L⁻¹) using all three methods. Decolorization of dye was analyzed at mentioned pH in different time intervals (0, 5, 10, 15, 20, 25, 30 and 35 min) for the SE, SPE and SPEC techniques. The decolorization rate was the highest at pH=9.0 in all three methods, but the rate constant at SPEC was more than the others (Figure 5).

This suggests that by using the photocatalyst, the amount of electro chemical reactions increases in the surface of electrodes [21]. In all of the electro chemical processes, pH shows its effect in the reaction in two ways. First, it enhances the segregation of electron-hole pairs and produces more oxidative species which is considering as a dominant role [22, 23]. Second, pH might increase the adsorption of the anionic dye which enhances the decolorization efficiency to some extent [24].
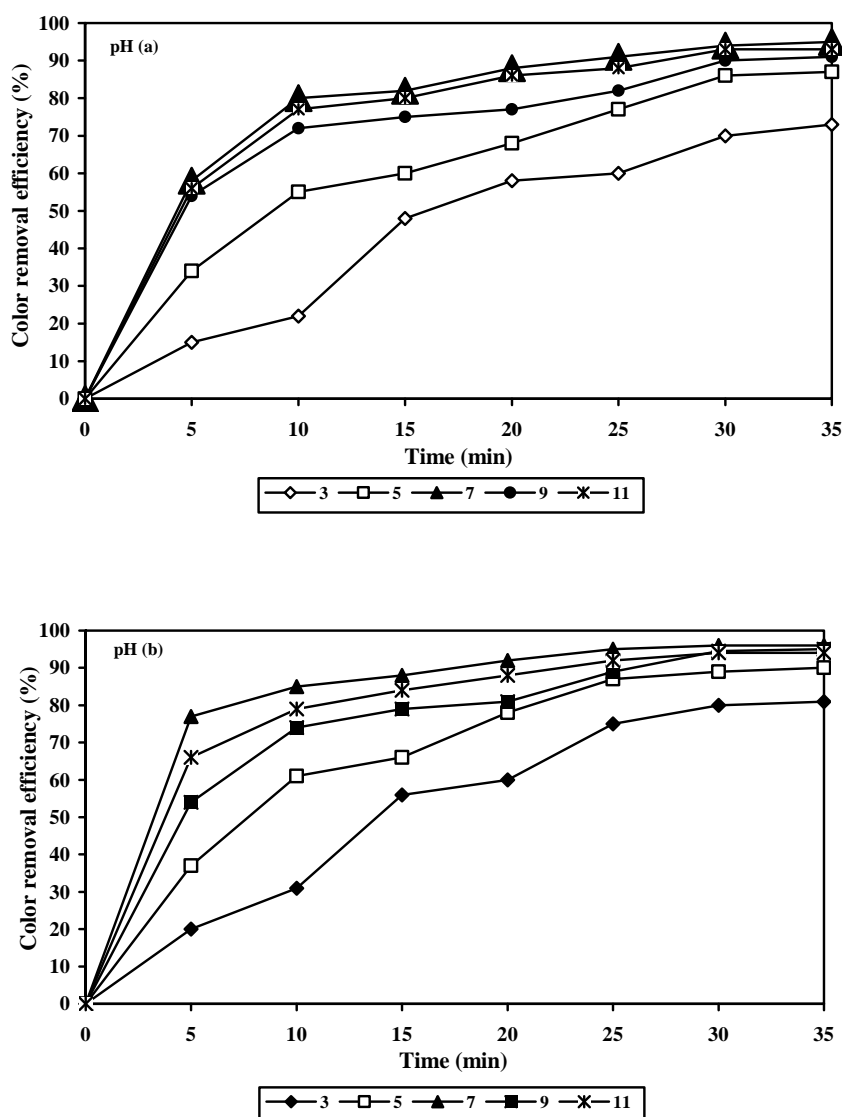

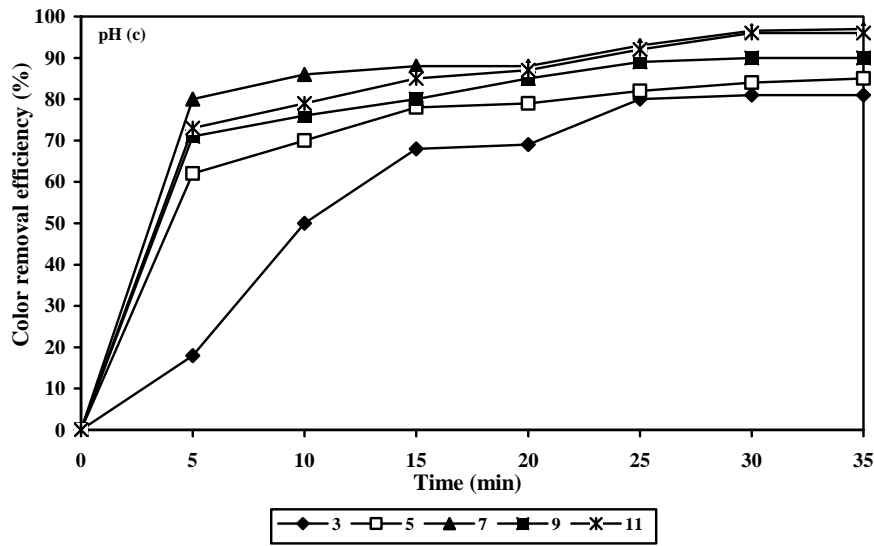**Figure 5:** Effect of pH on decolorization of AR88 for (a) SE, (b) SPE and (c) SPE.

Figure 5: Continued.

3.4. Effect of initial dye concentration

The decolorization efficiency of AR88 in SE, SPE, SPEC systems was evaluated as a function of initial dye concentration. In this practice, the initial dye concentration is varied from 30 to 250 mg L^{-1}. Figure 6 shows the effect of time and initial dye concentrations (30, 50, 100, 150, 200, 250 mg L^{-1}) on different mentioned processes. It is obvious that the initial concentration has important effect on the decolorization of dye in these processes [25].

Other investigations support this phenomenon as it is reported that the decolorization efficiencies in sonolysis, SE, SPE and SPEC extremely depend on the initial dye concentration [26]. It is obvious that by increasing the initial dye concentration, the percentage of degradated dye decreases and takes longer time to reach equilibrium. In other words, it is observed that for lower initial dye concentrations, decolorization is very fast. Faster decolorization of more dilute solution is attributed to the mobility of the dye molecules in dilute solution.
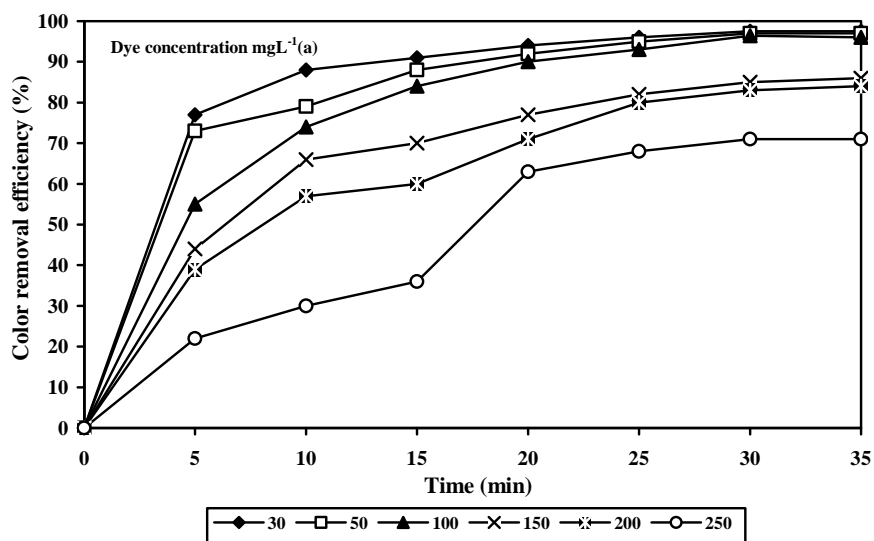

Figure 6: Effect of concentration on decolorization of AR88 in (a) SE, (b) SPE and (c) SPEC.
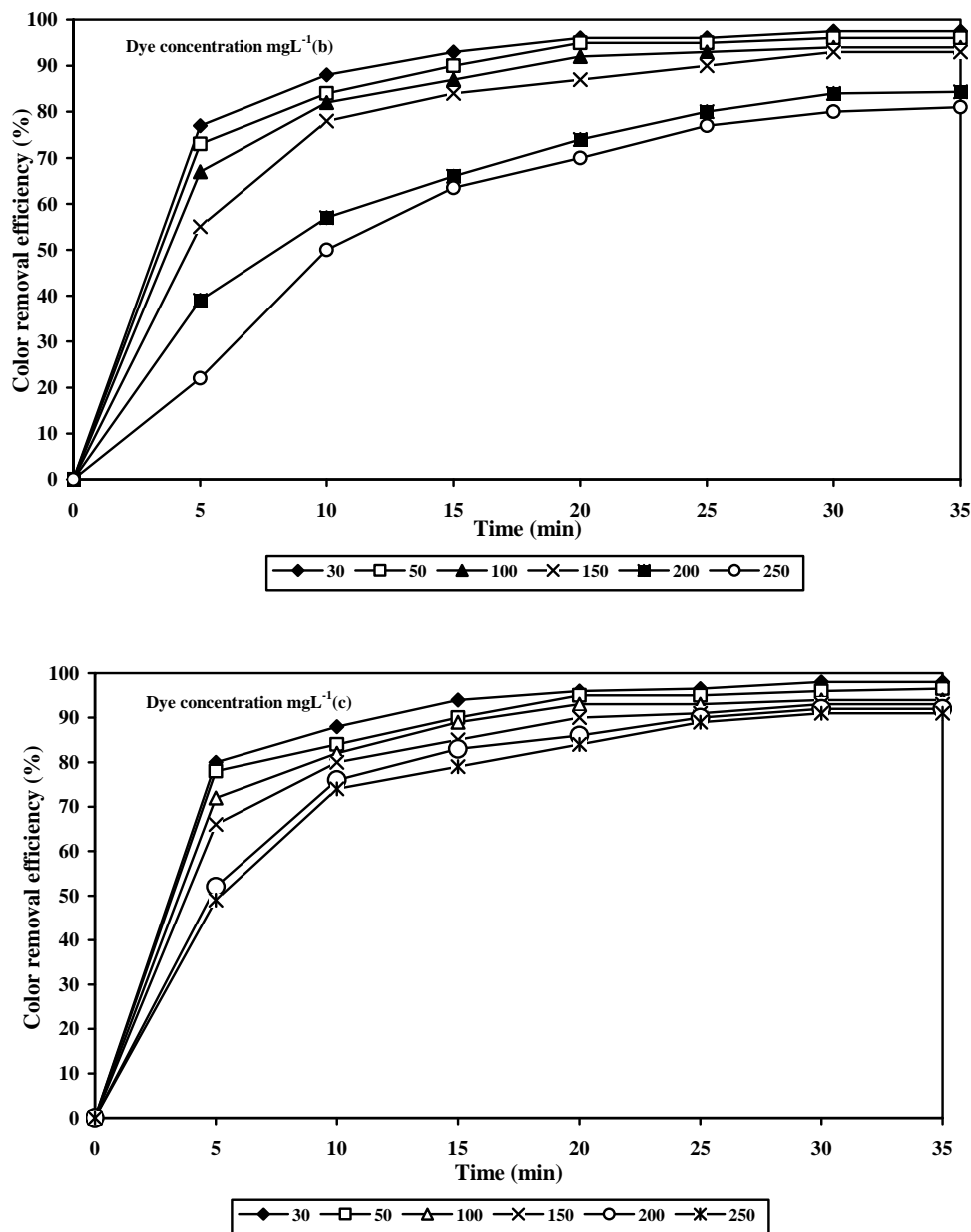
Figure 6: Continued.

From Figure 6, it is observed that the decolorization percentage of the dye for SPEC process reached 99% for initial concentration of 30 mg L^{-1}, 95% for 100 mg L^{-1} and 90% for 250 mg L^{-1} at the equilibrium.

3.5. Effect of electrolyte

In electro chemical studies, electrolyte type and concentration of supporting electrolyte is essential for increasing the conductivity of the solution. In this regard,

NaCl with the concentration of 5, 10, 15 and 20 mg L^{-1} were studied. It can be seen in Figure 7 that the color removal efficiency increases by increasing the electrolyte amount.

Because, by increasing the electrolyte, the ion density in the solution increases and the electrical resistance of the solution decreases, leading to higher conductivity of the solution and consequently decreasing the required voltage for a given current [27].
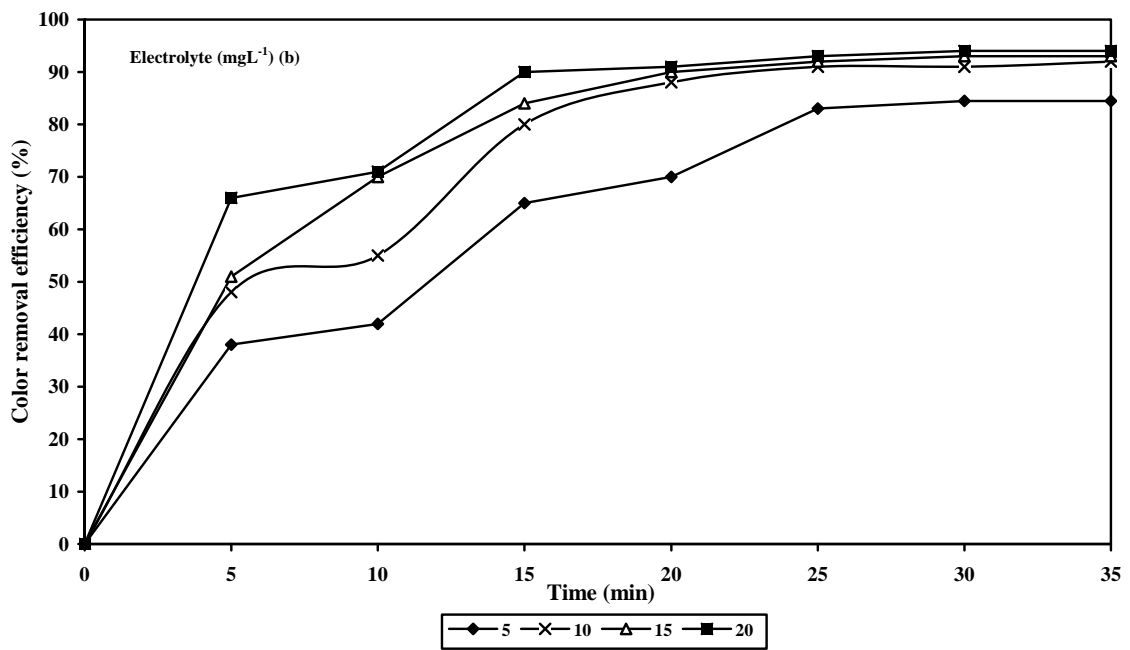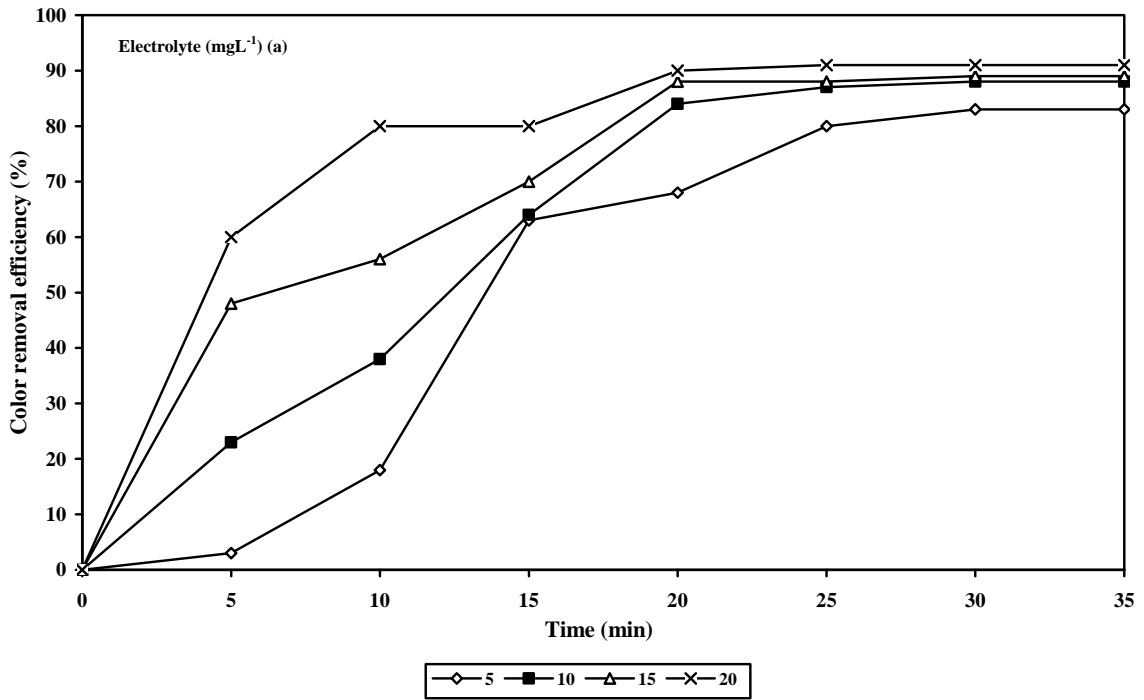
Figure 7: The effect of salt concentration on decolorization of AR88 in (a) SE, (b) SPE and (c) SPEC**.**
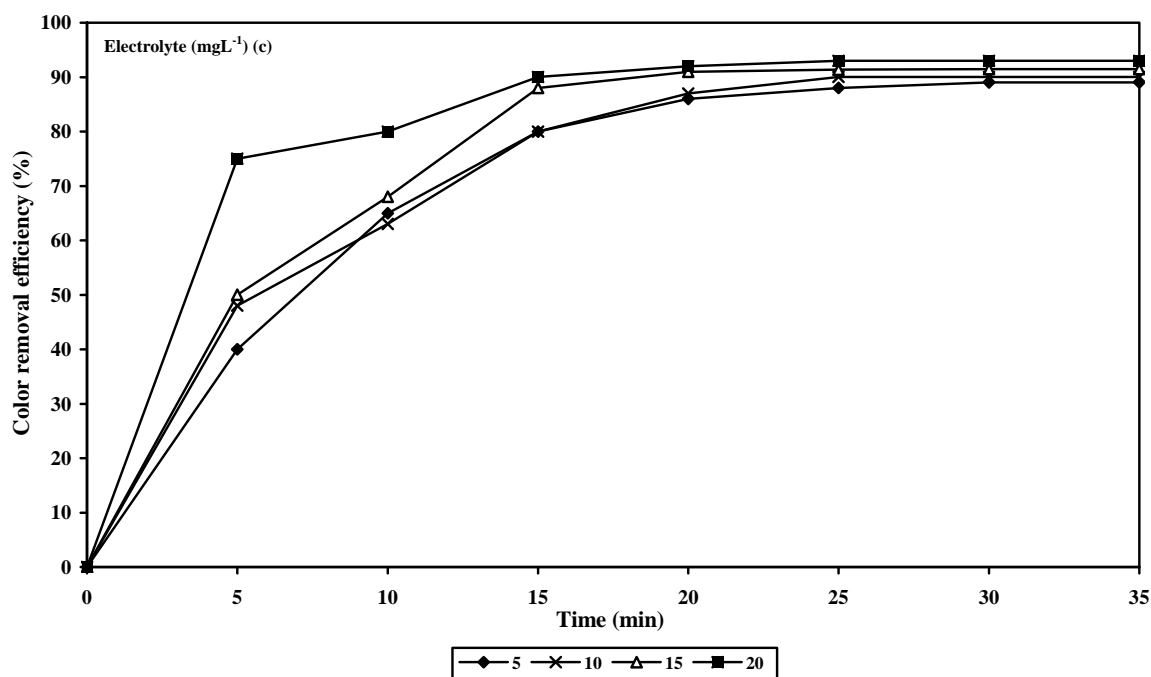
Figure 7: Continued.

NaCl is usually used for increasing the conductivity of water and wastewater that affects faradic result, cells voltage and energy consumption in electro chemical cell.

The increases of water conductivity using NaCl have also other advantages. It is noted that the absence of electrolyte can never lead to optimum situation in terms of energy consumption. The optimum energy consumption depends on the added NaCl. From the energy point of view, it is known that adding electrolyte can be useful for electro chemical, photo electro chemical and photo electrolysis processes except for very low current densities while, the energy doubles without adding NaCl in the case of higher current density. Current density will be 320 mA in the case of 15 mg L^{-1} NaCl. On the other hand, the energy consumption decreases by adding NaCl that is cost effective [28]. Therefore, the addition of NaCl can be used as an adjustable parameter that depends on the operator's goals such as maximizing the removal coefficient and decreasing the energy consumption.

3.6. Characterization and analysis

3.6.1. SEM and XRD analyses

The surface texture of TiO_2 was analyzed using the SEM technique. As can be seen in Figure 8(a), the particles are uniformly distributed without being agglomerated. Furthermore, the surface texture of the $Ni-TiO_2$ was determined by SEM before and after the SPEC process.

Figure 8(b) shows a porous structure with the micropores having amorphous edges. It can be seen from Figure 8(c) that the pores are blocked. This is an indicator of the adsorption of dye molecules onto the surface of $Ni-TiO_2$ particles during SPEC process.

Further, in order to investigate the effect of Ni doping on crystal structure of TiO_2, the X-ray diffraction (XRD) technique was applied. XRD measurements (Figure 9) were carried out in the range of $2\theta =10-80°$. The detected major peaks for the modified $Ni-TiO_2$ and unmodified TiO_2 samples appeared to be the same, but the intensities of the peaks were found to be significantly reduced in the case of $Ni-TiO_2$. In addition, peak broadening was noticed, which might be related to grain refinement resulting from doping.
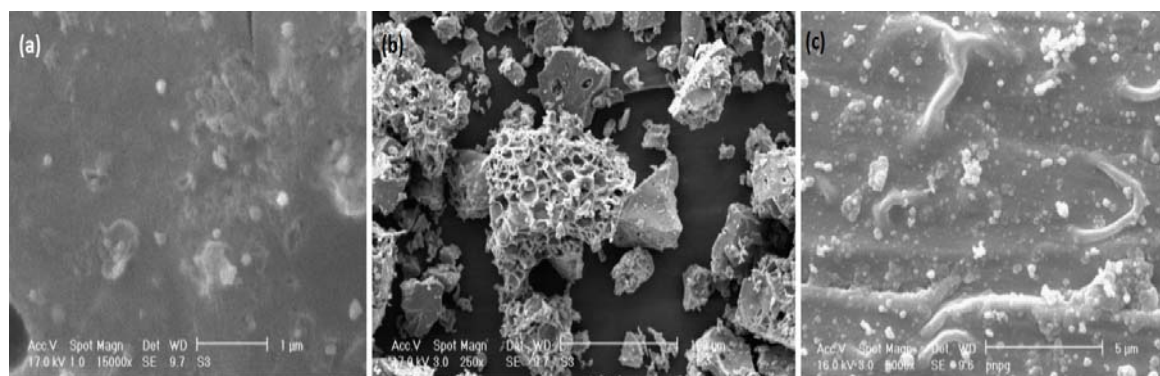
Figure 8: SEM image of (a)TiO_2, (b)original Ni-TiO_2, and (c) Ni-TiO_2 dyed by Acid Red 88**.**
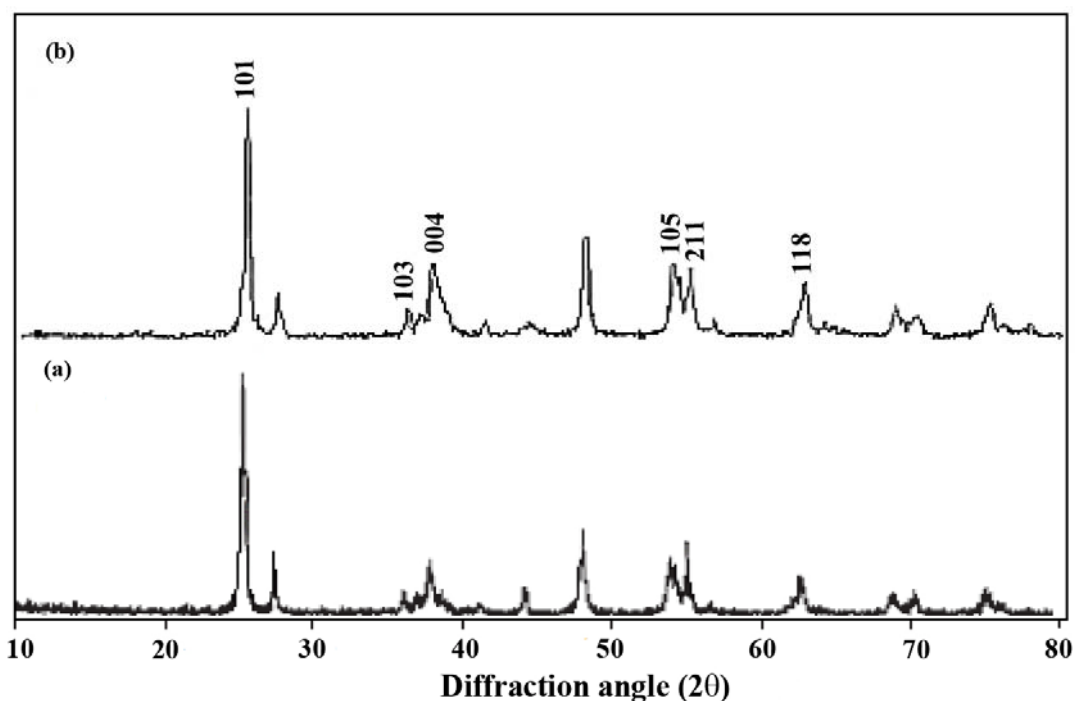

Figure 9: XRD spectra of (a)TiO_2 and (b) Ni-TiO_2**.**

It is believed that part of Ni has penetrated into TiO_2, and Ni ions were distributed uniformly in the interstices of semiconductor crystalline structure. Finally, no mixed phase was detected between Ni and Oxygen which may be due to the low loading (2%) of Nickel.

3.6.2. HPLC analysis

For HPLC analysis, AR88 dye solution was prepared by dissolving the commercial sample in acetonitrile HPLC grade and deionized water.

The analysis was carried out in triplicate for 20 min [29, 30, 31]. As shown in Figure 10, dye decolorization is identified by HPLC measurement in three methods in time intervals of 10, 20, 30 and 60 min.

Upon the injection of the initial solution, a well-developed peak emerged at the retention time of 3.5 min. However, 10 min after starting the reaction time, two peaks were observed, indicating the decomposition of the dye and the formation of a group of intermediates.

The findings represent the best results for SPEC procedure that all intermediates are eliminated after 60 min. The chromatogram also reveals that the concentration of these compounds was insignificant after an hour of treatment.

#

3.6.3. The mechanism of SPEC

Based on the results, it is possible to propose a pathway for the degradation of Acid Red 88 during the PEC process (Figure 11). To explain the process, the radical hydroxyl attacked the carbon atom bearing the dye leakage, leading to cleavage of the C–N bond and the generation of naphthalene-2-ol, 4-hydroxy-phthalicacid, and naphthalene-1-sulfonic acid.

Two transformation products were 3-sulfo-benzoic acid and benzene. If the SPEC process continues, these organic compounds will change into CO_2 and H_2O.
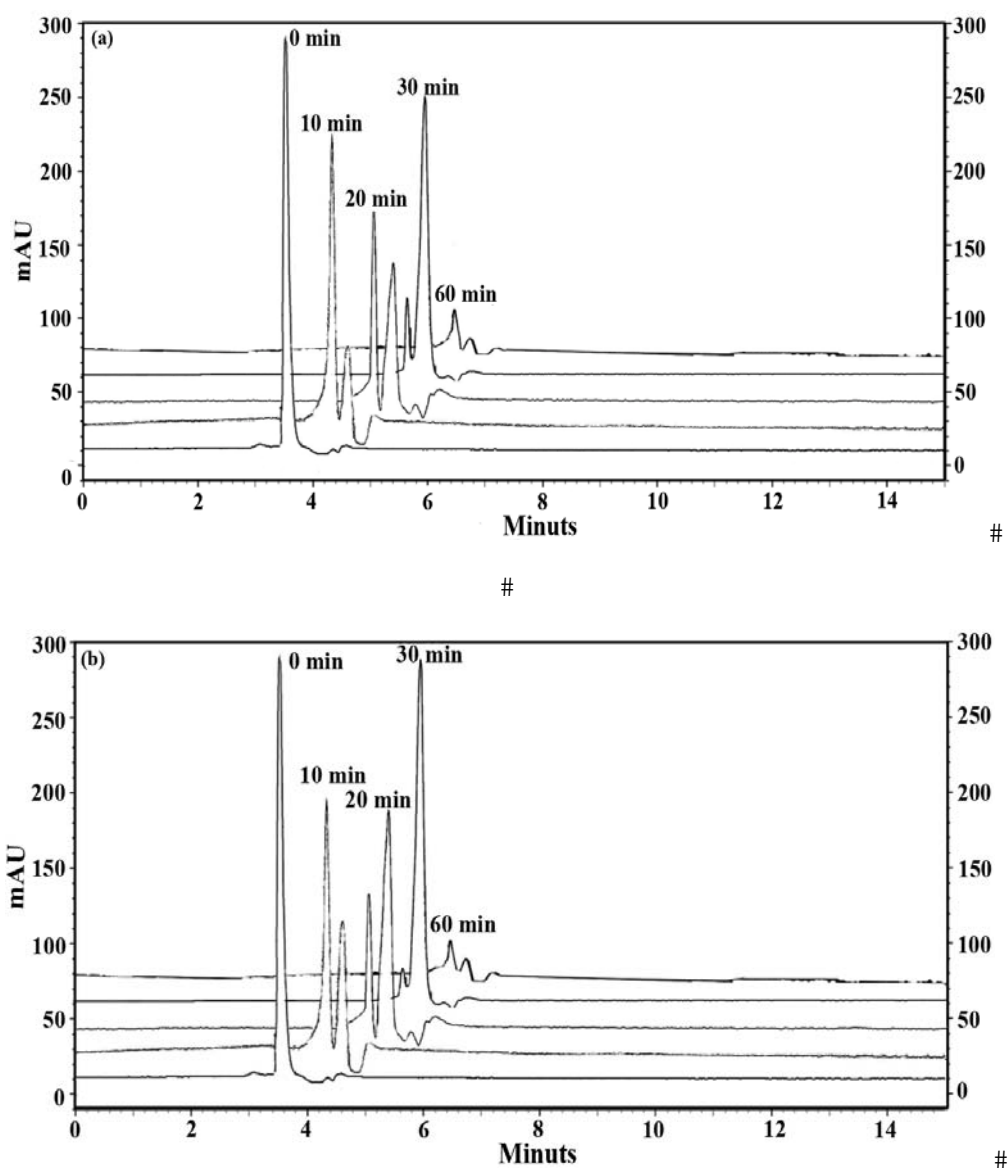
Figure 10: HPLC chromatograms at different dye decolorization time for (a) SE, (b) SPC and (c) SPEC.
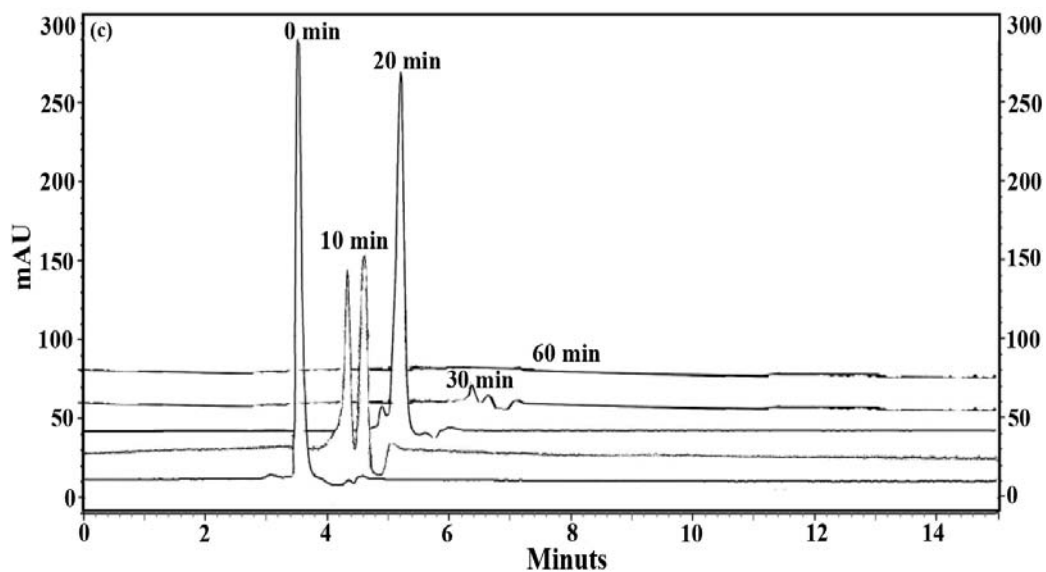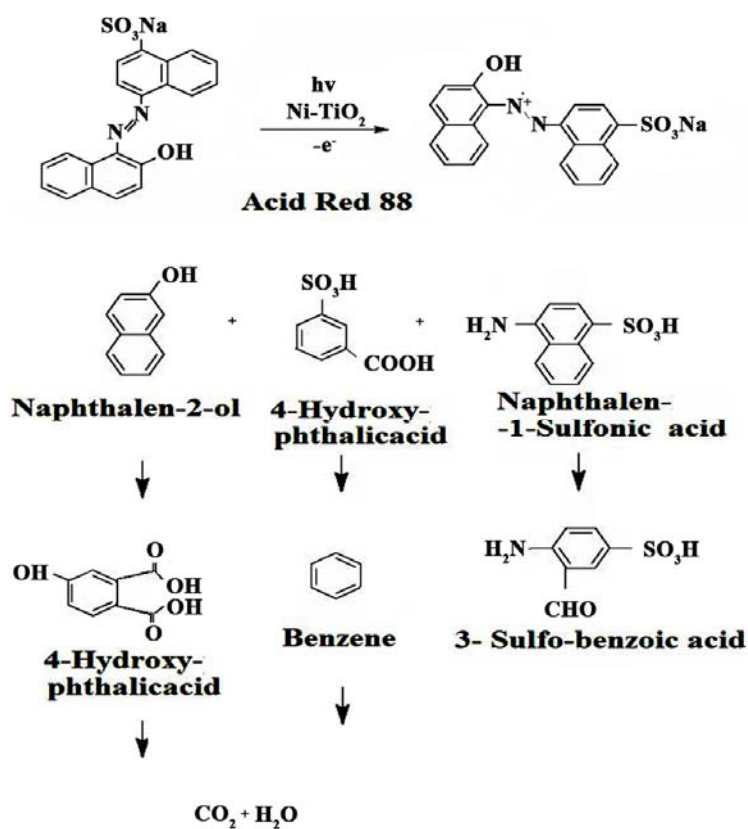
Figure 10: Continued.

Figure 11: The proposed mechanism for the SPEC.

4. Conclusion

Sonoelectrochemical method and its combination to photolytic and photocatalytic procedure were applied to study AR88 decolorization. The effect of different parameters such as current density, initial pH, dye concentration and electrolyte amount were optimized in these methods. An extraordinary synergetic effect was observed in SPEC technique. HPLC analysis carried out for SE, SPE and SPEC systems was a remarkable proof to spectrophotometric measurements. The results were satisfactory leading to high efficiency greater than 98% in 30 min for current density of 100 A m^{-2}, pH 9 and dye concentration of 30 mg L^{-1}.

5. References

1. T. Poursaberi, M. Hassanisadi, F. Nourmohammadian. Application of synthesized nanoscale zero-valent iron in the treatment of dye solution containing basic Yellow 28, *Prog. Color Colorants Coat.,* 5(2012), 35-40.

2. M. E. Olya, H. Aleboyeh, A. Aleboyeh, Decomposition of a diazo dye in aqueous solutions by KMnO$_4$/UV/H$_2$O$_2$ process, *Prog. Color Colorants Coat.,* 5(2012), 41-46.

3. M. N. Chong, B. Jin, C. W. K. Chow, C. Saint, Recent developments in photocatalytic water treatment technology: a review, *Water Res.,* 44(2010), 2997-3027.

4. A. Sakalis, D. Ansorgova, M. Holcapek, P. Jandera, A. Voulgaropoulos, Analysis of sulphonated azo dyes and their degradation products in aqueous solutions treated with a new electrochemical method, *Intern. J. Environ. Anal. Chem.,* 84(2004), 875-888.

5. K. Venkataraman, The analytical chemistry of synthetic dyes. Wiley, New York, 1997.

6. L. Wang, L. Zhu, W. Luo, Y. Wu, H. Tang, Drastically enhanced ultrasonic decolorization of methyl orange by adding CCl$_4$, *Ultrason. Sonochem.* 14(2007), 253-258.

7. D. E. Kritikos, N. P. Xekoukoulotakis, E. Psillakis, D. Mantzavinos, Photocatalytic degradation of reactive black 5 in aqueous solutions: effect of operating conditions and coupling with ultrasound irradiation, *Water Res.,* 41(2007), 2236-2246.

8. W. Baran, E. Adamek, A. Makowski, The influence of selected parameters on the photocatalytic degradation of azo-dyes in the presence of TiO$_2$ aqueous suspension, *Chem. Eng. J.,* 145(2008), 242-248.

9. M. R. Hoffmann, S. T. Martin, W. Choi, Environmental application of semiconductor photocatalysis, *Chem. Rev.,* 95(1995), 69-96.

10. C. C. Sun, T. C. Chou, Kinetics and mechanism of photoelectrochemical oxidation of nitrite ion by using the rutile form of a TiO$_2$/Ti photoelectrode with high electric field enhancement, *Ind. Eng. Chem. Res.,* 37(1998), 4207-4214.

11. P. A. Carneiro, M. E. Osugi, J. J. Sene, M. A. Anderson, M. V. B. Zanoni, Evaluation of color removal and degradation of a reactive textile azo dye on nanoporous TiO$_2$ thin-film electrodes, *Electrochim. Acta,* 49(2004), 3807-3820.

12. J. Li, L. Zheng, L. Li, Y. Xian, L. Jin, Fabrication of TiO$_2$/Ti electrode by laser-assisted anodic oxidation and its application on photoelectrocatalytic degradation of methylene blue, *J. Hazard. Mater.,* 139(2007), 72-78.

13. N. J. Bejarano-Pe´rez, M. F. Sua´rez-Herrera, Sonophotocatalytic degradation of congo red and methyl orange in the presence of TiO$_2$ as a catalyst, *Ultrason. Sonochem.*, 14(2007), 589-595.

14. S. Kaur, V. Singh, Visible light induced sonophotocatalytic degradation of Reactive Red dye 198 using dye sensitized TiO$_2$, *Ultrason. Sonochem.,* 14(2007), 531-537.

15. Y. Ding, C. Yang, L. Zhu, J. Zhang,# Photoelectrochemical activity of liquid phase deposited TiO$_2$ film for degradation of benzotriazole, *J. Hazard. Mater.,* 175(2010), 96-103.

16. K. W. Kim, E. H. Lee, Y. J. Kim, M. H. Lee, D. W. Shin, A study on characteristics of an electrolytic–photocatalytic reactor using an anode coated with TiO$_2$, *J. Photochem. Photobiol. A,* 161(2003), 11-20.

17. G. Li, J. Qu, X. Zhang, J. Ge. Electrochemically assisted photocatalytic degradation of Acid Orange 7 with β-pbo$_2$ electrodes modified by TiO$_2$, *Water Res.,* 40(2006), 213-220.

18. Z. Zhang, Y. Yuan, L. Liang, Y. Cheng, H. Ding, G. Shi, Sonophotoelectrocatalytic degradation of azo dye on TiO$_2$ nanotube electrode, *Ultrason. Sonochem.,*

15(2008), 370-375.

19. E. Valatka, Z. Kulesius. TiO$_2$-mediated photoelectrochemical decoloration of methylene blue in the presence of peroxodisulfate, *J. Appl. Electrochem.,* 37(2007), 415-420.

20. G. Li, J. Qu, X. Zhang, J. Ge, Electrochemically assisted photocatalytic degradation of Acid Orange 7 with β-pbo$_2$ electrodes modified by TiO$_2$, *Water Res.,* 40(2006), 213-220.

21. J. Gong, C. Yang, W. Pu, J. Zhang, Liquid phase deposition of tungsten doped TiO$_2$ films for visible light photoelectrocatalytic degradation of dodecyl-benzenesulfonate, *Chem. Eng. J.,* 167(2011), 190-197.

22. J. Zhang, B. Zhou, Q. Zheng, J. Li, J. Bai, Y. Liu, W. Cai, Photoelectrocatalytic COD determination method using highly ordered TiO$_2$ nanotube array. *Water Res.,* 43(2009), 1986-1992.

23. X. Quan, X. Ruan, H. Zhao, S. Chen, Y. Zhao. Photoelectrocatalytic degradation of pentachlorophenol in aqueous solution using a TiO$_2$ nanotube film electrode, *Environ. Pollut.,* 147(2007), 409-414.

24. D-R. Liu, Y-S. Jiang, G-M. Gao. Photocatalytic degradation of an azo dye using N-doped NaTaO$_3$ synthesized by one-step hydrothermal process, *Chemosphere,* 83(2011), 1546-1552.

25. M. Valnice, B. Zanoni, J. J. Sene, M. A. Anderson. Photoelectrocatalytic degradation of Remazol Brilliant Orange 3R on titanium dioxide thin-film electrodes, *J.*

Photochem. Photobiol. A., 157(2003), 55-63.

26. Z. Bao-xiu, L. Xiang-zhong, W. Peng, Degradation of 2,4-dichlorophenol with a novel TiO$_2$/Ti-Fe-graphite felt photoelectrocatalytic oxidation process, *J. Environ. Sci.,* 19(2007), 1020-1024.

27. M. E. Osugi, K. Rajeshwar, E. R. A. Ferraz, D. P. de Oliveira, Â.R. Araújo, M. Valnice, B. Zanoni, Comparison of oxidation efficiency of disperse dyes by chemical and photoelectrocatalytic chlorination and removal of mutagenic activity, *Electrochim. Acta.,* 54(2009), 2086-2093.

28. A. Aleboyeh, N. Daneshvar, M. B. Kasiri, Optimization of C.I. Acid Red 14 azo dye removal by electrocoagulation batch process with response surface methodology, *Chem. Eng. Process.,* 47(2008), 827-832.

29. Y. Ding, C. Yang, L. Zhua, J. Zhang, Photoelectrochemical activity of liquid phase deposited TiO2 film for degradation of benzotriazole, *J. Hazard. Mater.,* 175(2010), 96-103.

30. F. M. M. Paschoal, M. A. Anderson, M. V. B. Zanoni, The photoelectrocatalytic oxidative treatment of textile wastewater containing disperse dyes, *Desalination,* 249(2009), 1350-1355.

31. P. A. Carneiro, D. P. Oliveira, G. A. Umbuzeiro, M. V. B. Zanoni, Mutagenic activity removal of selected disperse dye by photoeletrocatalytic treatment, *J. Appl. Electrochem.,* 40(2010), 485-492.